

CFD STUDY ON THE INTERACTION BETWEEN WATER SPRAYS AND LONGITUDINAL VENTILATION IN TUNNEL FIRES

Patricio Valdés Gacitúa

IDIEM - Investigación, Desarrollo e Innovación de Estructuras y Materiales
Plaza Ercilla 883
Santiago, Región Metropolitana, 8320000, Chile
e-mail: patricio.valdes@idiem.cl

ABSTRACT

The current research has been conducted to study and analyze the interaction of the water spray produced by the water mist system and the smoke layer in tunnel fires where the longitudinal ventilation is operating. The study has been carried out through several computational simulations in the CFD package denominated “Fire Dynamics Simulator”, following the technical features of facility built at Wuhan University. Different scenarios and system configurations were performed following the indications of Wuhan University to compare the impact of the droplet diameter, the flow rate, and the injection pressure in the flow interaction. Besides, the longitudinal ventilation has been performed to obtain the back-layering phenomena for the fire scenarios. The sensitivity analysis has been executed in the nozzles simulations to obtain the mesh cell size and the number of water droplets.

As a result, it is possible to argue that the interaction of the water spray in to the smoke layer with the longitudinal ventilation, resulting from the analysis in the smoke layer height, smoke temperature, velocity field, water flux distribution and heat was absorbed by water droplets.

Keywords: Watermist, Tunnel, Fires, Smoke, Longitudinal, Ventilation, Interaction, FDS, droplets, CFD.

INTRODUCTION

As it is widely known that the smoke in tunnels causes most of the damage to the properties as well as casualties. Therefore, controlling the smoke in tunnels is a problem that needs to be solved. Longitudinal ventilation systems are commonly used in tunnels [Nie, Fang & Tang, 2017]. The smoke management strategy in a longitudinal ventilation system provides a safe place for firefighting and rescue in the upstream of the fire. This system may break the smoke stratification inside of the tunnel. If the smoke stratification is broken, the evacuation and rescue through the tunnel will be obscured and will have a big impact in saving lives. When the ventilation velocity is smaller than the required critical velocity, there will be smoke back-layering.

The stratification of the smoke back layer would also be important for the evacuation and firefighting. Application of Spray-based Fixed Fire Fighting Systems (WFFFS) in tunnels has been a controversial topic for decades. One of the reasons is that the stratification of the smoke layer could be destroyed by WFFFS. Therefore, the fixed water systems installed in the tunnel could generate an impact in the smoke layer and stratification of the hot gases.

METHODOLOGY

As the main objective of the present project is to model the interaction between the water spray nozzle and the smoke layer in tunnels, several simulations in the CFD package (Fire Dynamics Simulator) will be computed and analyzed.

In this chapter the general procedure followed in each simulation and analysis is given. It will be described the experimental work and the simulations, as well as how the sensitivity analysis is performed.

General Procedure

As the first step of the procedure, the experimental work in the mid-scale tunnel test is reviewed and described. The technical features of the mid-scale test tunnel are described, in order to maintain the same conditions in the simulations of CFD package.

Due to the results of the experiments in the mid-scale test tunnel have not been carried out, there is no results available before starting the simulations in the FDS. Thus, the simulations conducted in the FDS will be a "Blind Simulations".

After reviewing the mid-test tunnel experimental set up, the fire modelling has been modelled following the specifications of the experimental set up. According to this procedure, it is possible to decrease the testing computational time, due to that the fire is modelled without the ventilation system and the spray nozzle system. This method allows to review it in less time than running the complete set up.

The next step, the ventilation numerical modelling will be modelled according the technical features indicated in the mid-test tunnel experimental set up. Besides, the information provided by the fire modelling will be coupled to the ventilation numerical modelling.

Following the previous step, the water spray nozzle will be modelled in several stages in order to generate a sensitivity analysis regarding to the cell size of the mesh and the number of particle that have been injected through the nozzle. Then, the fire simulation at the tunnel is coupled with the nozzles network and calculated in the FDS, obtaining the interaction between the smoke layer and the water spray.

The last step of this research is to conduct the simulation of the fire in the tunnel, the longitudinal ventilation and the nozzles network interacting each other. Therefore, the three models will be coupled and computed in the same simulation in order to obtain the interaction of the water droplets and the smoke layer in an environment of longitudinal velocity.

Experimental Work

The following description is a brief summary of the experimental work of the mid-scale tunnel test. The technical features and the description of the set-up is described in this **Error! Reference source not found.**

The mid-scale tunnel consists of a facility that contains a solid tunnel of masonry-concrete structure, with dimensions of 3 m wide, 2.2 m high and 30 m long. The fire will be located at the center of the tunnel in two pans containing the liquid fuel. The ventilation system consists in mechanical ventilation located in one of the opening of the tunnel, therefore it will be injected the fresh air from the outside into the tunnel, generating the back-layering phenomena.

The water nozzle system is distributed in two sides of the fire source and it is located at the ceiling of the tunnel (2.2 m height). The total number of nozzles is 30 (15 nozzles at each side of the fire) spaced

in rows of 3 nozzles. Each group of 15 nozzle is equipped with a manually water valve, in order to activate the group of nozzles together or separated in the experiment.

Three levels of water pressure have been adopted to test the nozzle system, which was 0.5 MPa, 0.7 MPa and 0.9 MPa. The technical features of the nozzles as the cone shaped region of discharge, the mean diameter of the droplets, among others, have been conducted in the laboratory of the Wuhan University and they are described in the **Error! Reference source not found.**

CFD Simulations

The CFD simulations that need to be performed will be computed in the FDS (Fire Dynamics Simulator) package. Since the results of the experimental mid-scale tunnel test were not available during the development of the current research, the CFD simulations can be classified as “Blind Simulations”. In other words, the set-up of the CFD simulations have been performed in order to represent in the best way the mid-scale tunnel conditions.

Therefore, the “blind simulations” that will be configured and computed in the CFD package, aim at obtaining results that, in future experiments, they could be compared and analyzed with the results of the test in the mid-scale tunnel.

EXPERIMENTAL WORK

Tunnel Characteristics

The tunnel, where the test will be performed, it is called a mid-scale test tunnel and the dimensions are 3 m wide, 2.2 m high and 30 m long. The walls and the ceiling of the tunnel have been built in masonry concrete. The mechanical and thermal features are presented in the Table 1 and Table 2.

Table 1: Tunnel’s mechanical and thermal properties

Density	Heat Conductivity	Specific Heat
kg/m ³	W/(m*K)	kJ/(kg*K)
1900	1.1	1.05

Table 2: Air Properties Considered

Air Density	Cp	T° Ambient
kg/m ³	kJ/kg °K	°K
1.204	1.005	293

Fire Load

The fire in the mid-scale test tunnel will comprise the combustible liquid Methyl Alcohol (Methanol). The total number of pool fire will be two, where each pan has dimensions of 0.82 m long and 0.61 m wide (0.5 m²), as is indicated in the Figure 1.

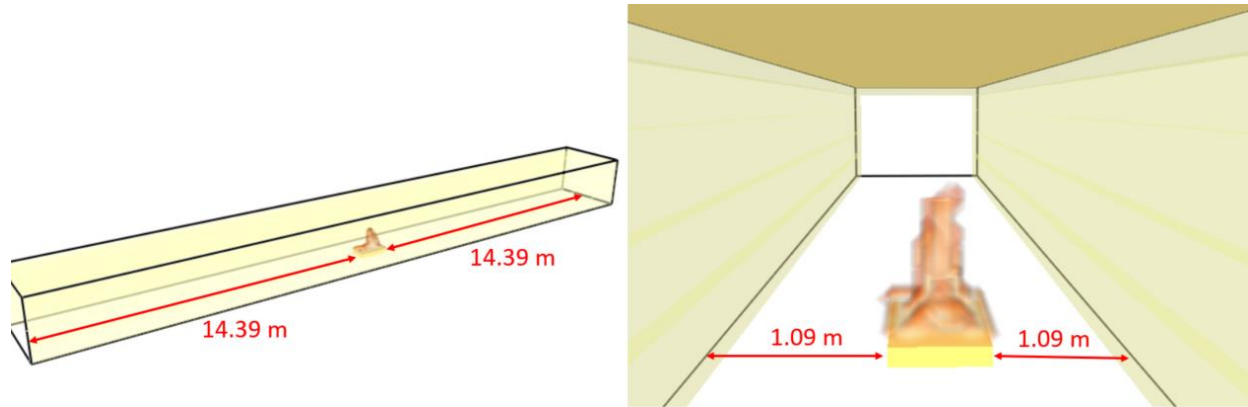


Figure 1: Fire Location

Heat Release Rate

The Heat Release Rate (HRR) has been calculated according to the values of mass loss rate presented in the equation 1 and calculated according following.

$$HRR = \eta * \dot{m}_c * \Delta H_c \quad \text{Eq. 1}$$

Where HRR is the heat release rate in J/s or Watt, correspond to the combustion efficiency factor with a value of 0.9 and ΔH_c is the heat of combustion of Methanol with a value of 19.83 kJ/g.

Ventilation System

The ventilation system that is installed in the mid-scale test tunnel can be classified as a longitudinal system and contains 3 rotational fans, located at one of the opening sides of the tunnel.

Between the air rotational fans and the inside of the tunnel, there is a honeycomb structure that creates a uniform velocity across the tunnel. The characteristics of the fans are presented in the Table 3.

Table 3: Ventilation Parameters

Flow Rate	m ³ /h	9500
Rotational Speed	rpm	1450
Voltage	Volt	380
Motor Power	Watt	370

According to the theoretical development and estimations computed by the mid-scale test, the tunnel without the water mist system operating requires a longitudinal velocity of 1.29 m/s to generate the back-layering phenomena. So, the adjustment of the ventilation system and the fans in the set-up of the mid-scale test, requires that the mean velocity measured in the cross section of the tunnel should be 1.368 m/s (according the set-up of the mid-scale tunnel test).

Water Spray

The water system used for the experiment inside of the tunnel will be arranged with 30 nozzles distributed in two grids across the ceiling of the tunnel. Each grid contains 15 nozzles located at 4.5 m away from the fire. The configuration of the nozzle grid is arranged in 5 rows separated at 1.5 m each other, while the distance between the nozzles correspond to 0.75 m. The technical features of the nozzles that will be implemented in the test are described as follows.

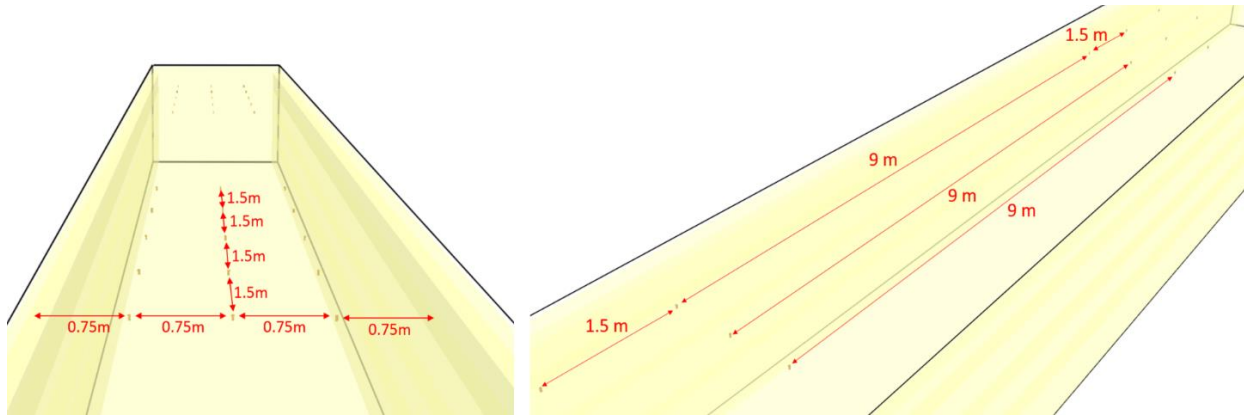


Figure 2: Water Spray system Location

The droplet diameter distribution was measured by a laser particle sizer, where the energy dispersed by the droplets is captured in the electronic receiver.

The empirical measurement of the droplet diameter distribution agrees well with the Rosin-Rammler curve, where the mass fraction (Y_d) of the liquid droplets with the diameter greater than d is computed by the following equation.

Where \bar{d} is the mean diameter, n is the distribution parameter and the cumulative mass fraction smaller than d is represented by $(1 - Y_d)$.

$$Y_d = e^{-\left(\frac{d}{\bar{d}}\right)^n} \quad \text{Eq.2}$$

Table 4: Water Characteristics

Water Pressure	MPa	0.5	0.7	0.9
Water Flow Rate	l/min	0.92	0.97	1.055
Discharge Coefficient	lpm/Mpa ^{0.5}	0.411	0.366	0.351
Angle of Spray	° Angle	77	80	84
Mean Diameter	µm	152	135	122
Dv 50	µm	137	120	112
Distribution Parameter	n	3.343	3.21	5.065

NUMERICAL SET-UP

Tunnel Fire & HRR

The fire, developed in the tunnel, has been considered as a well-ventilated fire. Therefore, it is possible to obtain the yields of fire products as well as chemical, convective, and radiative heats of combustion from the handbook of SFPE. The yield products of carbon monoxide are 0.001 g/g and the chemical composition of the Methyl alcohol correspond to CH₃OH.

The fire will be computed until the model reach a steady state condition, so, it is considered an “unlimited” fuel as a correct assumption for this research. Besides, the radiation model will not be activated. The HRR considered correspond to 384.1 kW.

Fire Geometry & Mesh

The pool fires will be located inside and in the centre of the mid-scale tunnel according to Figure 3.

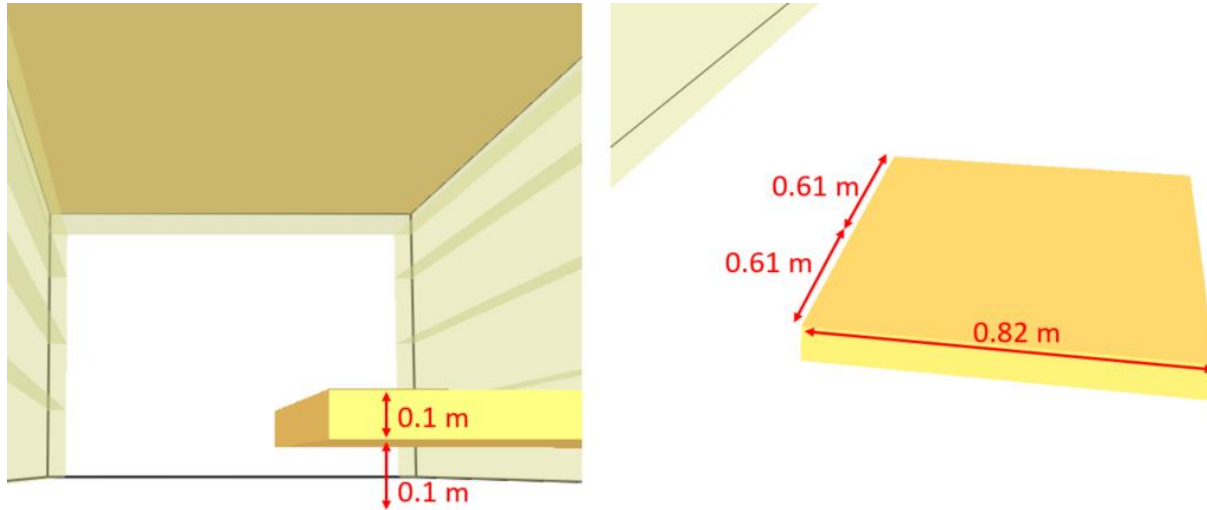


Figure 3: Fire Geometry

For simulations involving buoyant plumes, a measure of how well the flow field is resolved is given by the non-dimensional expression $\frac{D^*}{\delta x}$ where D^* is a characteristic fire diameter and δx is the nominal size of a mesh cell.

$$D^* = \left(\frac{Q}{\rho C T \sqrt{g}} \right)^{\frac{2}{5}} \quad \text{Eq. 3}$$

Where \dot{Q} is heat release rate of the fire is, ρ is the air density at ambient temperature, C correspond to the air specific heat, T is the ambient temperature and g is the acceleration due to gravity. In a sensitivity analysis (Lehtimaki, 2017), sponsored by the U.S. Nuclear Regulatory Commission, the $D^*/\delta x$ value ranges between 4 and 16.

In order to generate a sensitivity analysis regarding to the cell size, three different mesh will be configured, one of them will be coarse mesh with a value of $\Delta x \approx 8$, then the fine mesh will have a value of $\Delta x \approx 12$ and finally the refined mesh will contain a value of $\Delta x \approx 16$.

The Table 5 present the values for the theoretical calculations of the cell size for the mesh according to the methodology described before

Table 5: Sensitivity analisys according FDS developer

HRR (kW)	D^*	Coarse Mesh		Fine Mesh		Refined Mesh	
		x (mm)	$D^*/\delta x$	x (mm)	$D^*/\delta x$	x (mm)	$D^*/\delta x$
384.1	0.655	0.082	8	0.055	12	0.041	16

Due to the geometry of the simulation, the cell size has been adapted and adjusted in order to match the entire cell within the computational domain as it is possible to see in Table 6.

Table 6: Total mesh for different cell-size

Coarse Mesh				
x (m)	Nº Cell X	Nº Cell Y	Nº Cell Z	Total Cell
0.075	40	40	32	51200

Fine Mesh				
x (m)	Nº Cell X	Nº Cell Y	Nº Cell Z	Total Cell
0.05	60	60	48	172800

Refined Mesh				
x (m)	Nº Cell X	Nº Cell Y	Nº Cell Z	Total Cell
0.04	75	75	60	337500

Radiation Modelling

According to the background of fire in tunnels, the main heat transfer mechanism corresponds to the convection. This influences not only the interaction between the droplets and the smoke layer, but also the fire dynamics in tunnel. Therefore, the radiation model will not be activated to save computational time in the simulations.

Turbulence Model

The turbulence model corresponds to the Deardorff model. This agreement was reached because there is not enough information to modify the default turbulence model. Besides, the default settings are adequate settings for the cases that will be simulated. In addition, no synthetic turbulence (SEM) was added to the model, due to the honeycomb that is installed in the mid-scale tunnel perform a laminar air flow.

Longitudinal Ventilation

According the technical features of the mid/scale tunnel and the ventilation system, the honeycomb installed creates a transversal uniform velocity profile. This profile will be modelled in the FDS creating a vent at the extreme of the tunnel, supplying the air required to generate the back-layering phenomena. The supply of air will be considered as the entire area of the tunnel opening. The area that corresponds to the walls and ceiling are subtracted from the air inlet area (Figure 4).

According to the experimental data that is indicated by the experimental mid-scale tunnel test, the critical velocity measured to produce the back-layering phenomena will correspond to 1.368 m/s.

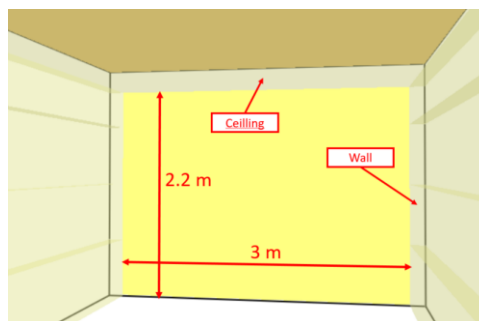


Figure 4: Inlet Air Dimensions

Water Spray

Spray Boundary Conditions

As is presented earlier the initial droplet velocity can be calculated as follows.

$$K = \frac{\dot{V}_w}{\sqrt{\Delta P}} \quad \text{Eq. 4}$$

Then the flow \dot{V}_w is measured in liter per minute, the relative pressure P at the nozzle is in Bar or MPa and the discharge coefficient K is in L/m/bar^{1/2}. In Table 7 the results for the initial velocity are presented where the nozzle orifice area is considered as well as the water flow rate and the discharge coefficient.

Table 7: Initial Velocity Calculation

Water Pressure	Water Flow Rate		Discharge Coefficient	Nozzle Orifice Diameter	Nozzle Orifice Area	Initial Velocity	Dv 50
	l/min	m3/min					
Mpa	l/min	m3/min	lpm/Mpa ^{0.5}	mm	m2	m/s	µm
0.5	0.92	0.00092	0.411	1.2	1.13094E-06	13.558	137
0.7	0.97	0.00097	0.366	1.2	1.13094E-06	14.295	120
0.9	1.055	0.001055	0.351	1.2	1.13094E-06	15.548	112

The spray angles, according to the experimental work are presented in the Table 8. It is possible to see that the angle of the spray of the nozzle increases as a function of the water pressure. The type of the water cone according to the table corresponds to full cone.

Table 8: Angle of the spray

Water Pressure	Water Flow Rate	Angle of Spray	
		θ min (°)	θ max (°)
Mpa	l/min		
0.5	0.92	0	38.5
0.7	0.97	0	40
0.9	1.055	0	42

Initial Droplet Size Diameter and Distribution

As it has been obtained through the Rosin-Rammler in the experimental work, the Dv 50 diameter is presented in the following table.

Table 9: Size and Distribution of Droplet

Water Pressure	Water Flow Rate	Dv 50
Mpa	l/min	µm
0.5	0.92	137
0.7	0.97	120
0.9	1.055	112

Volume Flux Angular Distribution as a Function of θ

For the modelling of the spray nozzle pattern shape, the pattern that has been chosen corresponds to the uniform pattern. The volume flux angular chosen to be applied in the simulation is the uniform distribution, due to its similarity to the water shape than the nozzle discharged in the experimental

work. Besides, there is no requirement to discharge more water in some special places; therefore, the uniform flux distribution is a good choice of water discharge shape.

Number of Particles

The default number of particles per second used in the modelling of sprinklers in the CDF package is 5000. Most of the researchers and studies that has been conducted in steady simulations were achieved with $1.0, 1.5$ and 2.0×10^5 particles per second for water mist nozzles (Lehtimaki, 2017).

Small particle count caused numerical instability when particles were hit to the hot surface. The higher flow rates aggravated the phenomenon. Therefore, to assess the sensitivity analysis required for the computational simulations, the number of particles that has been chosen to simulate the spray nozzle will correspond to 5000, 10000, 20000, 30000, 40000, 50000, 100000, 150000 and 200000.

Finally, according the results obtained in the simulations of the sensitivity analysis shown in the current research, the number of particles that will be configured and simulated in the rest of the simulations will be 100000 droplets.

Final Mesh

According to the results obtained in the sensitivity analysis, the mesh and cell size that will be used for the tunnel will be the re-fined mesh. The total number of cells that has been considered in the tunnel is shown in Table 10.

Table 10: Total Cell Number

Cell Size (m)	X Axe Length (m)	Y Axe Length (m)	Z Axe Length (m)	Total
0.04	30	3.32	2.4	3735000

As it is restricted by the FDS software that it is not possible to exceed 1.2 million cells per processor, the mesh for the tunnel presented in the Table 10 will be divided in 8 mesh with the same number of cells along the tunnel. Then, each mesh will be assigned to different cores of the HPC where the simulations will be solved (Figure 5).

Therefore, for the simulations of fire, fire & longitudinal ventilation, spray nozzles & fire, the mesh shown in the Table 10. As it is shown in the Figure 5, in the HPC it will be assigned 466875 cells per core.

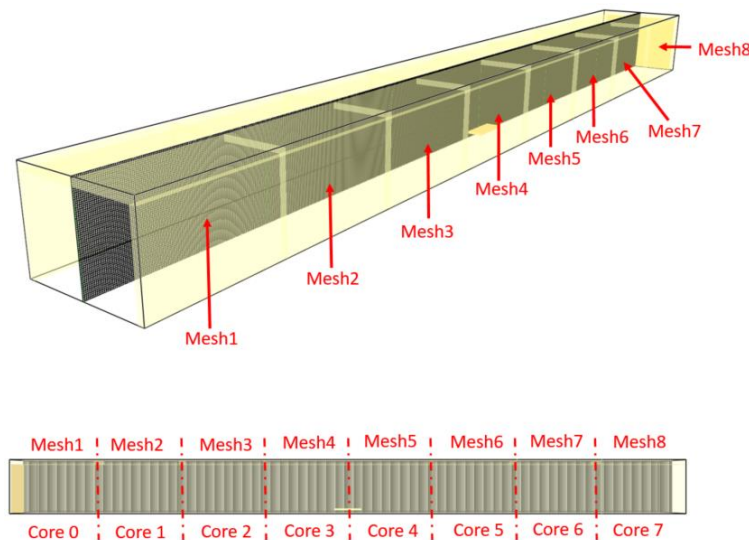


Figure 5: Mesh divided according Number of Cores

For the simulations of spray nozzles and fire with ventilation, the mesh cell size has been decreased from the re-fined mesh to the fine mesh. The reason is that the wall time (max time) of the HPC (Boerstlap, 2014) system is 72 hours, and if the re-fined mesh is used, the wall time is exceeded. Therefore, as it is possible to see in the sensitivity analysis of the present research, the fine mesh still presents a good accuracy and low deviation results.

Therefore, for the simulations of spray nozzles and fire with ventilation the cell size used is presented in the Table 11. The number of cores is maintained as is indicated in the Figure 5, using 239040 cells per core in the HPC.

Table 11: Total number of Cells

Cell Size (m)	X Axe Length (m)	Y Axe Length (m)	Z Axe Length (m)	Total
0.05	30	3.32	2.4	1912320

Modelling Time

To determine the time of modelling per each simulation, it is necessary to detect the time when the conditions inside of the tunnel are steady state in the whole domain. To assess the steady state condition, several measurements according to the list of simulations has been produced and described in the list of simulations in the present research.

Measurement and Post-Processing

The Figure 6 presents the velocity measurements points regarding to the water discharge of the nozzle. In the current research there were 2 types of velocity measurements, one of them correspond to the centerline velocity (green dots - Figure 6) and radial velocity at certain height (blue dots - Figure 6)

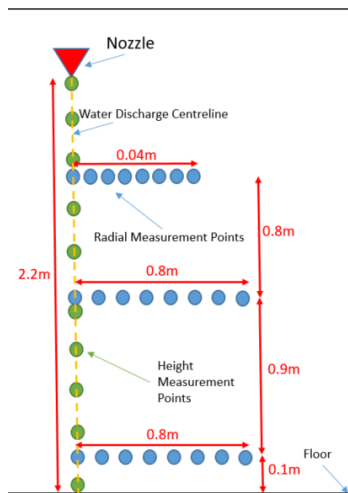


Figure 6: Measurement devices for centerline droplet velocity

The Figure 7 contain the measurement places for the smoke height.

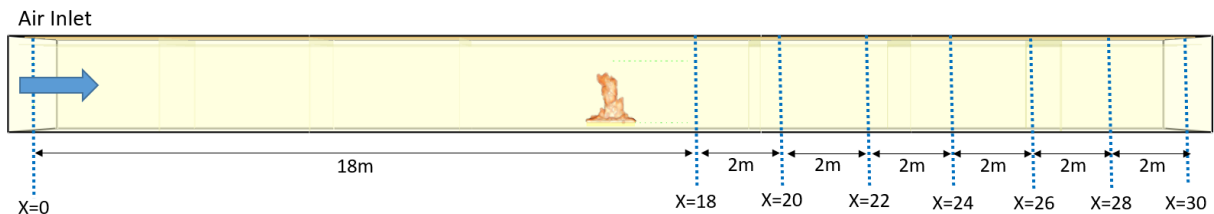


Figure 7: Measurement locations for smoke layer height

LIST OF SIMULATIONS

Several simulations were conducted regarding to the configuration and the set – up of the mid-scale tunnel test. Some of the simulations has been performed to assess a sensitivity analysis and the rest has been accomplished to fulfill the general analysis and make available comparisons and analysis between the scenario's results.

Gas-Phase

Fire

One scenario has been simulated to obtain the behavior of the fire inside in the tunnel and make available future comparison with ventilation or spray nozzles.

Fire & Ventilation

One scenario corresponding to the fire and the longitudinal ventilation was simulated without the interaction with spray nozzles, to compare with the results of the multi-phase simulations.

Multi-Phase

The multiphase stage corresponds to the simulations of the interaction between the single-phase stage and the spray nozzle network. In this stage also a sensitivity analysis will be performed to decrease the computational time.

Sensitivity Analysis

Two sensitivity analysis has been performed to determine the best cell size for the simulations and the number of water droplets corresponding to water mist system.

The first sensitivity analysis is regarding to the cell size of the mesh and it will be performed to select the best mesh according to the computational resources.

The second sensitivity analysis (after the first analysis) correspond to the number of the droplets exerted by a water mist system. The analysis has been modelled covering the range of the droplets exerted by a sprinkler (5000-10000) until the theoretical number of the water mist droplets (100000-200000).

Spray Nozzles & Fire

After the sensitivity analysis has been completed, three simulations have been performed to study in a general way the interaction between the spray nozzles and the ceiling jet produced by the fire.

Spray Nozzles & Fire with Longitudinal Ventilation

Three scenarios were conducted to obtain the results for the interaction between the fire, the longitudinal ventilation, and the operation of the spray nozzles. Each scenario contains the same variables as geometry, fire, and ventilation characteristics. The variable modified correspond to the pressure of the spray nozzle system.

Summary of Simulations

The following tables contain the summary of the simulations performed in the present research. Each simulation has been named with a tag, permitting to identify faster and better the characteristics and the configuration of the scenario.

The Table 12 present the simulations performed for the sensitivity analysis regarding with the mesh cell-size. The Table 13 present the simulations completed regarding to the sensitivity analysis of number of droplets. The Table 14 contains the general simulations performed for the research.

Table 12: Simulations performed for the sensitivity analysis of cell-size

Simulation Tag	Fire	Ventilation	Spray Nozzle		Mesh
			Activated	Pressure (MPa)	
1A	No	No	Yes	0,5	Coarse
2A			Yes	0,7	
3A			Yes	0,9	
1B	No	No	Yes	0,5	Fine
2B			Yes	0,7	
3B			Yes	0,9	
1C	No	No	Yes	0,5	Re-Fined
2C			Yes	0,7	
3C			Yes	0,9	

Table 13: Simulations performed for the sensitivity analysis of number of droplets

Simulation Tag	Fire	Ventilation	Spray Nozzle		Mesh	N° Droplets
			Activated	Pressure (MPa)		
3C-0	No	No	Yes	0,9	Re-Fined	5000
3C-05						10000
3C-06						20000
3C-07						30000
3C-08						40000
3C-09						50000
3C-1						100000
3C-2						150000
3C-3						200000

Table 14: Simulations performed for the main analysis

Simulation Tag	Stage	Fire	Ventilation	Spray Nozzle	
				Activated	Pressure (MPa)
-	Single-Phase	Yes	No	No	-
-		Yes	Yes	No	-
1C1	Multi-Phase	Yes	Yes	Yes	0,5
2C1		Yes	Yes	Yes	0,7
3C1		Yes	Yes	Yes	0,9

RESULTS & DISCUSSION

Gas-Phase

Fire

Based on the temperature at the tunnel's portal, the beginning of the steady state conditions start at 25 seconds after the beginning of the fire. Consequently, the total simulation of the fire alone inside the tunnel is simulated for 50 seconds.

As it is expected, the temperature is higher and closer to the fire location than places closer to the tunnel portals (Figure 8).

In addition, it is also possible to see that the smoke layer is thinner and closer to the portals of the tunnel, instead of being closer to the fire location, where it is thicker.

The height of the hot gases layer corresponds to approximately 0.7 m, so there is still 1.5 m free of smoke and hot gases inside of the tunnel (Graph 1).

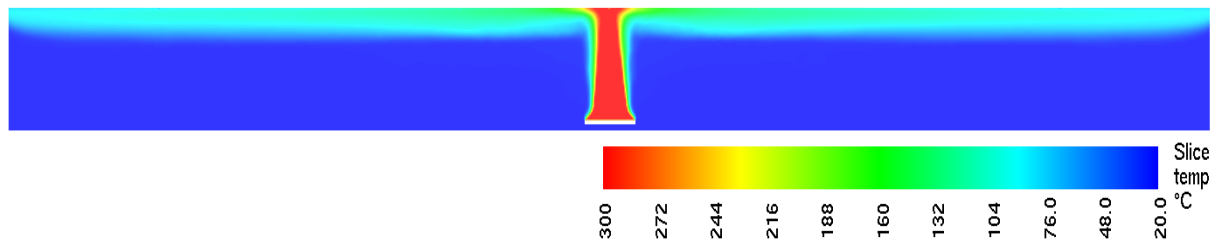
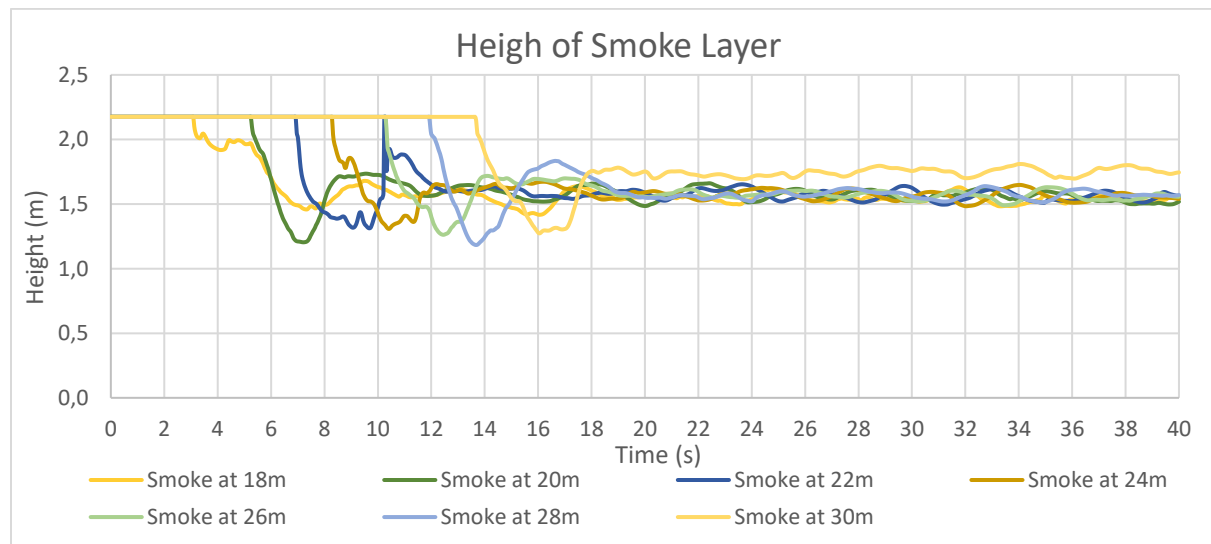


Figure 8: Longitudinal Side View of Temperature Slice



Graph 1: Smoke Height at Several Locations

Fire & Ventilation

It is possible to state that after the second 128, there is no back-layering distance in front of the fire anymore, and the whole smoke layer and hot gases are pushed to the other direction. The frontal part of the fire is completely clear and supported with fresh air after the second 128.

The Figure 9 contains the longitudinal temperature profile across the tunnel. As it is possible to see, the black color upstream of the fire location represents 20°C, so it can be assumed that there is fresh air in the tunnel, which is presented in the complete left part of the tunnel (considering the fire location as the center of the tunnel).

On the other hand, on the right side of the tunnel, it is possible to see the temperature profile, which now is thicker than the fire in the tunnel without the longitudinal ventilation. The temperature profile for the tunnel with the longitudinal ventilation is lower when the fire is burning without the longitudinal ventilation

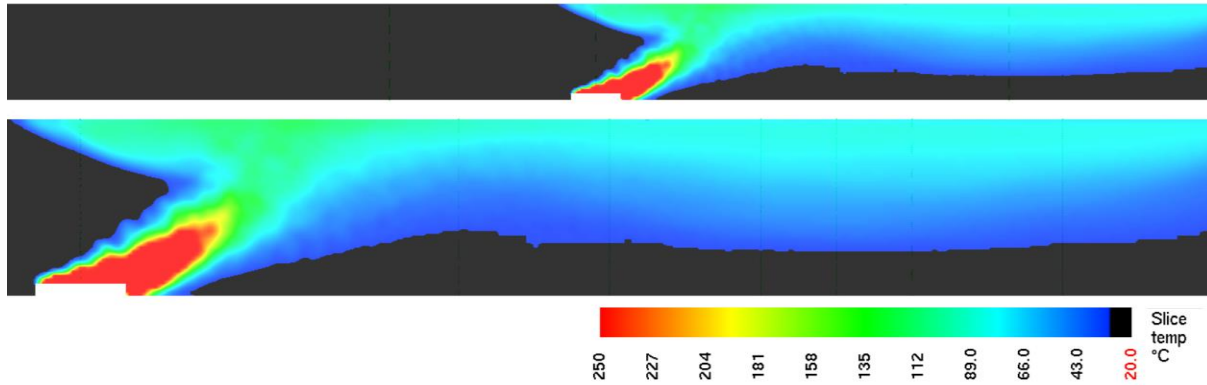
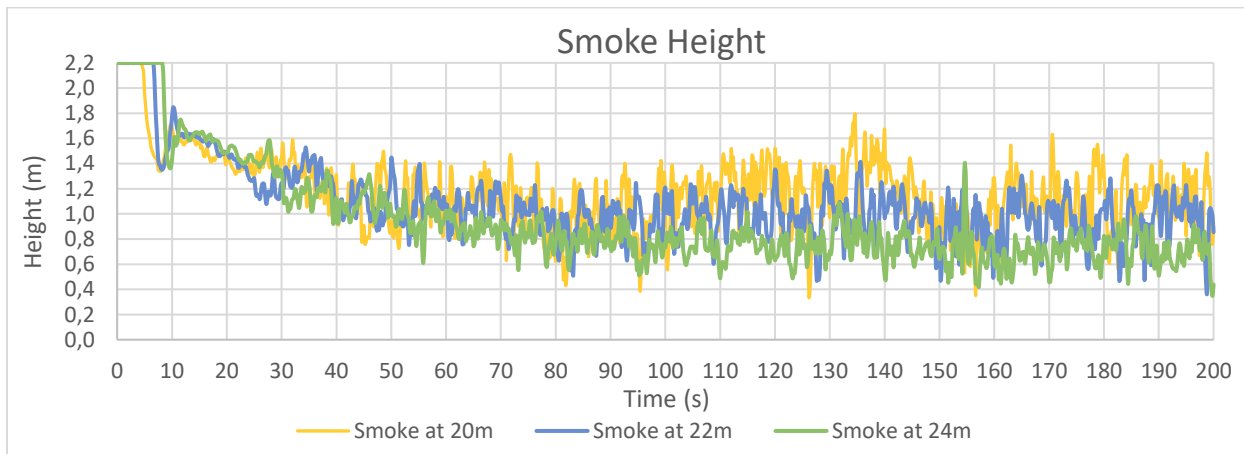
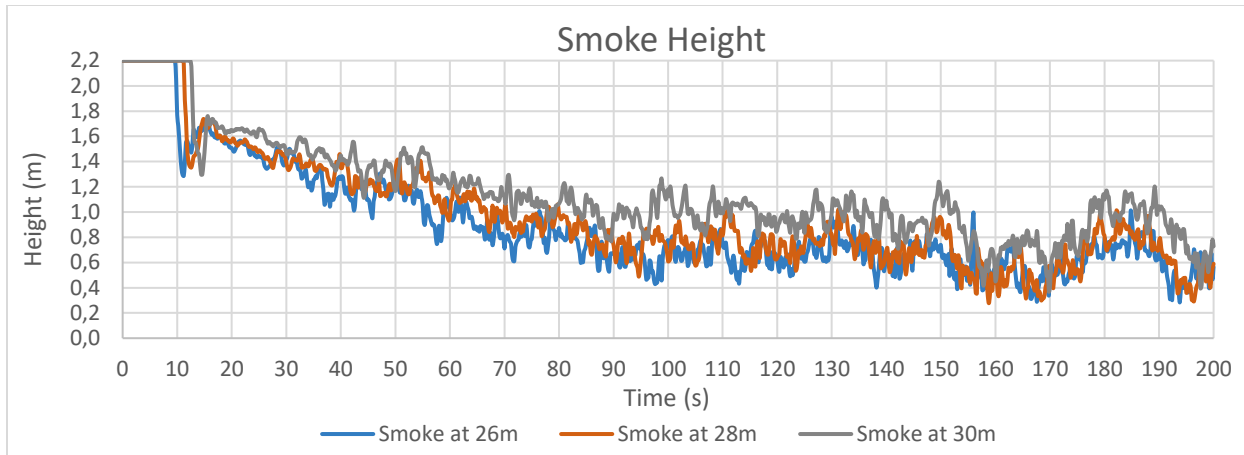


Figure 9: Longitudinal Side View of Temperature Slice

The plot of the height of the smoke layer is presented in Graph 2 & Graph 3. The points of measurement were placed at 20m, 22m, 24m, 26m, 28m and 30m away from the tunnel portal where the air was injected (left tunnel portal).



Graph 2: Smoke height at different tunnel locations



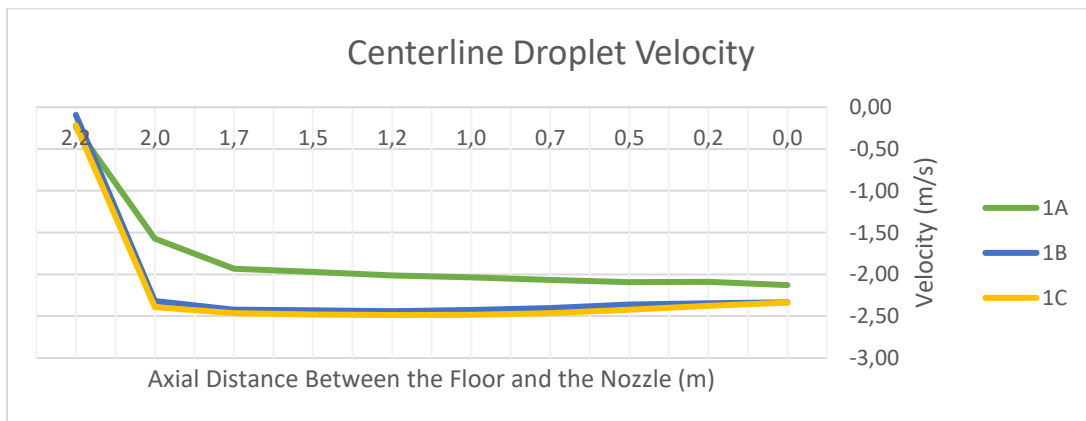
Graph 3: Smoke height at different tunnel locations

Multi-Phase

Sensitivity Analysis

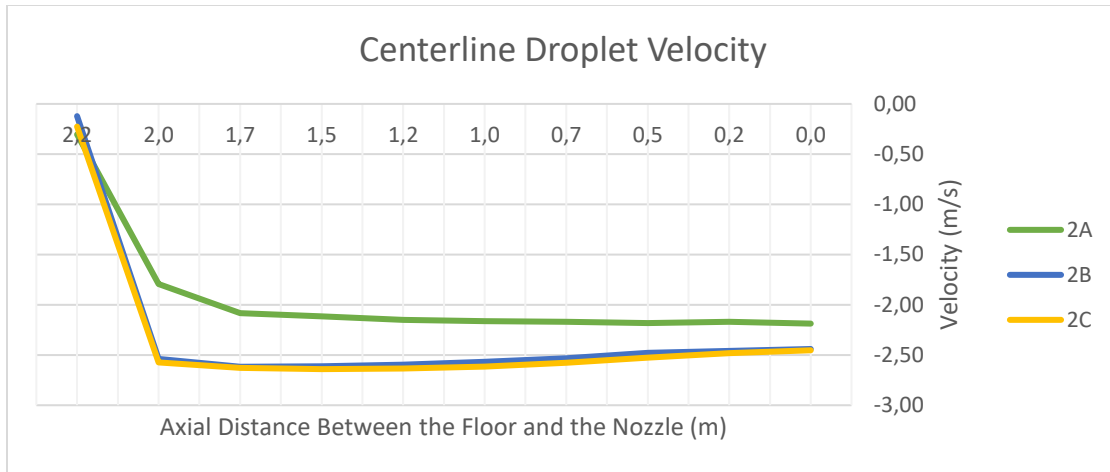
The time of modelling of the water discharged by the nozzle will be determined regarding the stabilization of the values of the water flux output. It is possible to state that the values of the water flux start to become stable from the second 6.8 of the simulation. There a simulation of 10 seconds will be considered.

Graph 4 presents the numerical value of the centerline velocity according the height between the nozzle and the ground for 0.5 MPa in three different cell-size mesh. The values obtained in the coarse mesh are 18.01% lower than the re-fined mesh, while the fine mesh present values of velocity 2.51% lower than re-fined mesh (Graph 4).



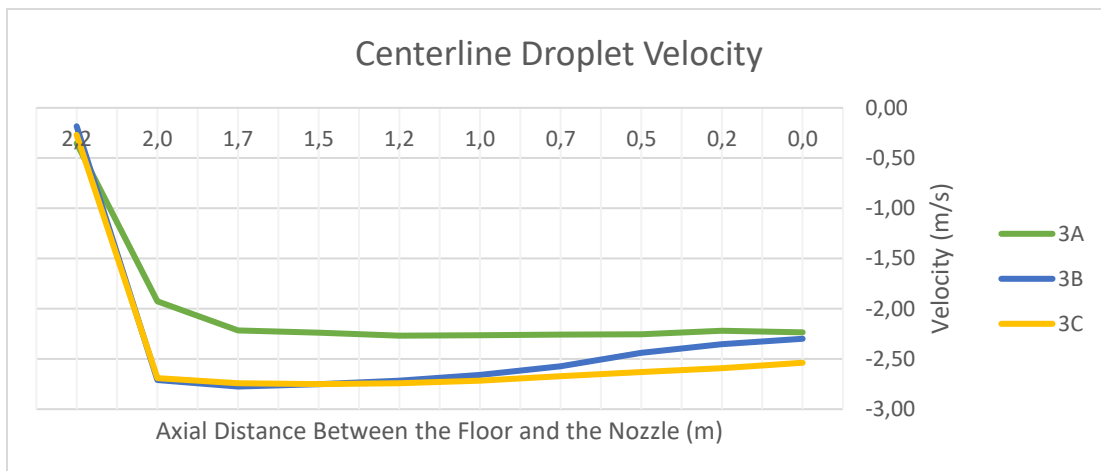
Graph 4: Centerline Droplet Velocity @ 0.5 MPa and several Cell-size

the Graph 5 presents the numerical value of the centreline velocity according the height between the nozzle and the ground for 0.7 MPa in three different cell-size mesh. The values obtained in the coarse mesh are 17.29% lower than the re-fined mesh, while the fine mesh present values of velocity of 1.65% under estimated in relation to the re-fined mesh (Graph 5).



Graph 5: Centerline Droplet Velocity @ 0.7 MPa and several Cell-size

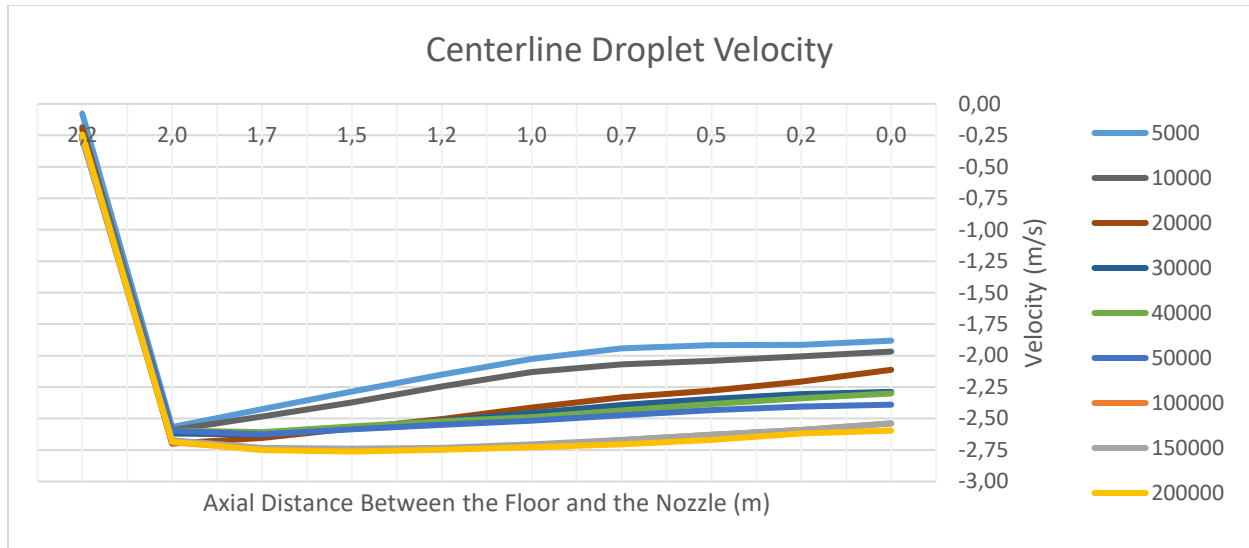
the Graph 6 present the numerical value of the centreline velocity according the height between the nozzle and the ground. The values obtained in the coarse mesh are 16.87% lower than the re-fined mesh, while the fine mesh present values of velocity 3.6% under estimated regarding to the re-fined mesh (Graph 6).



Graph 6: Centerline Droplet Velocity @ 0.9 MPa and several Cell-size

The number of the droplets that has been modelled is detailed in the Table 13 which cover the range of the droplets exerted by a sprinkler (5000-10000) until the theoretical number of the water mist droplets (100000-150000). Consequently, it will be possible to see the impact of the differences between the types of water discharge devices and therefore, save computational time.

As the information presented in the Graph 7, the centerline velocity is plotted as function of the height of the nozzle in each number of droplet. It is possible to observe that the values of the velocity droplet in the area closer to the floor do not present a big difference in the numerical values among the several simulations. So, it is presented a good estimation of the centerline velocity as a terminal velocity of the droplet in every case.



Graph 7: Centerline Droplet Velocity from Different N° of Droplets

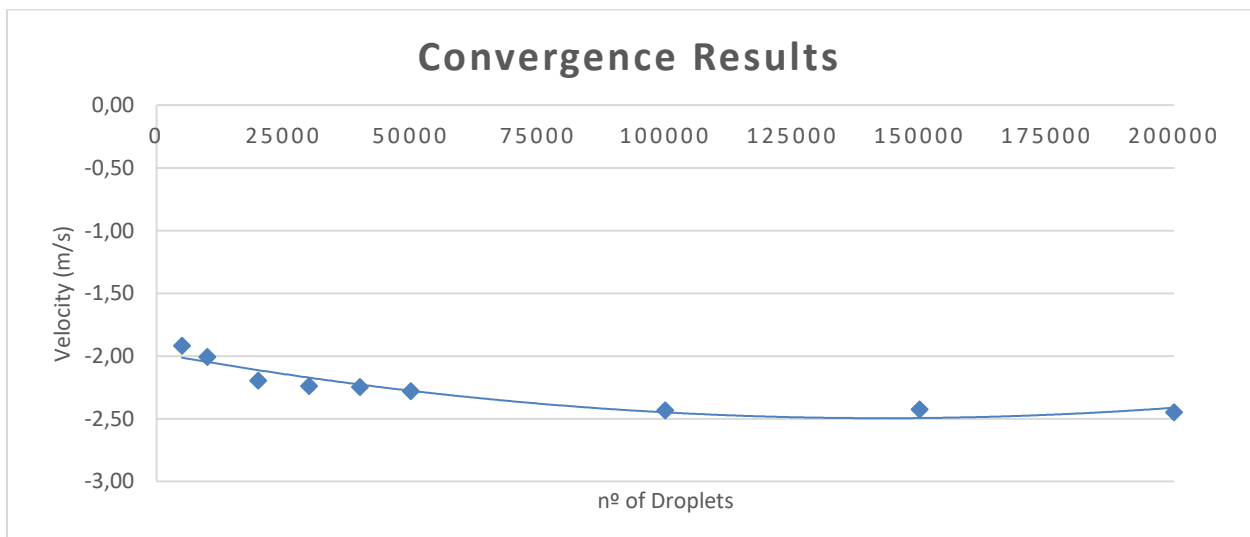
On the other hand, the lower numbers of particles present a strong underestimation in comparison with the higher numbers of droplets when measuring the centerline velocity from the nozzle until the 2 meters away (Graph 7).

The Table 15 contains the variation in the numerical results of the centerline velocity averaged across the whole domain.

Table 15: Variation of Velocity numerical values

N° of Droplets	5000	10000	20000	30000	40000	50000	100000	150000	200000
% of Variation	21.7	18	10.3	8.56	8.24	6.85	0.67	0.9	-

The Graph 8 contains the variations in the averaged centerline velocity in function of the number of droplets. As it is possible to see, the values of the variations decrease when the number of droplets of 100000 is reached. As a result, it is possible to state that the convergence of the values is presented at 100000.



Graph 8: Convergence Results of Centerline Velocity

Spray Nozzles & Fire

After 7 seconds of the simulation the values of the water flux do not present a strong variation; therefore, it will be considered a total simulation time of 50 seconds, where the first 35 seconds corresponds to the fire and the last 15 seconds relates the spray nozzle activation.

Figure 10 contains the longitudinal view of temperature in the tunnel without the nozzle operation and after the operation of each nozzle configuration. As it is possible to see, there is a decrement in the temperature downward of the fire in each nozzle configuration. Besides, the injection of the water in the tunnel (more specific in the ceiling where the smoke is stratified) produces that hot gases descend from the ceiling into the fresh air zone (black zone indicated in Figure 10)

It is important to note that the temperature of the hot gases, after the interaction with the water, is still hot enough to maintain the buoyancy. Therefore, the decrease of the smoke layer is produced due to the vertical momentum exerted by the water cones of the nozzles, as it is possible to see close to the tunnel portal in Figure 10. On the other hand, the results present small differences between each configuration, where it is possible to see that the lowest injection pressure generate a higher decrease of the hot layer gases.

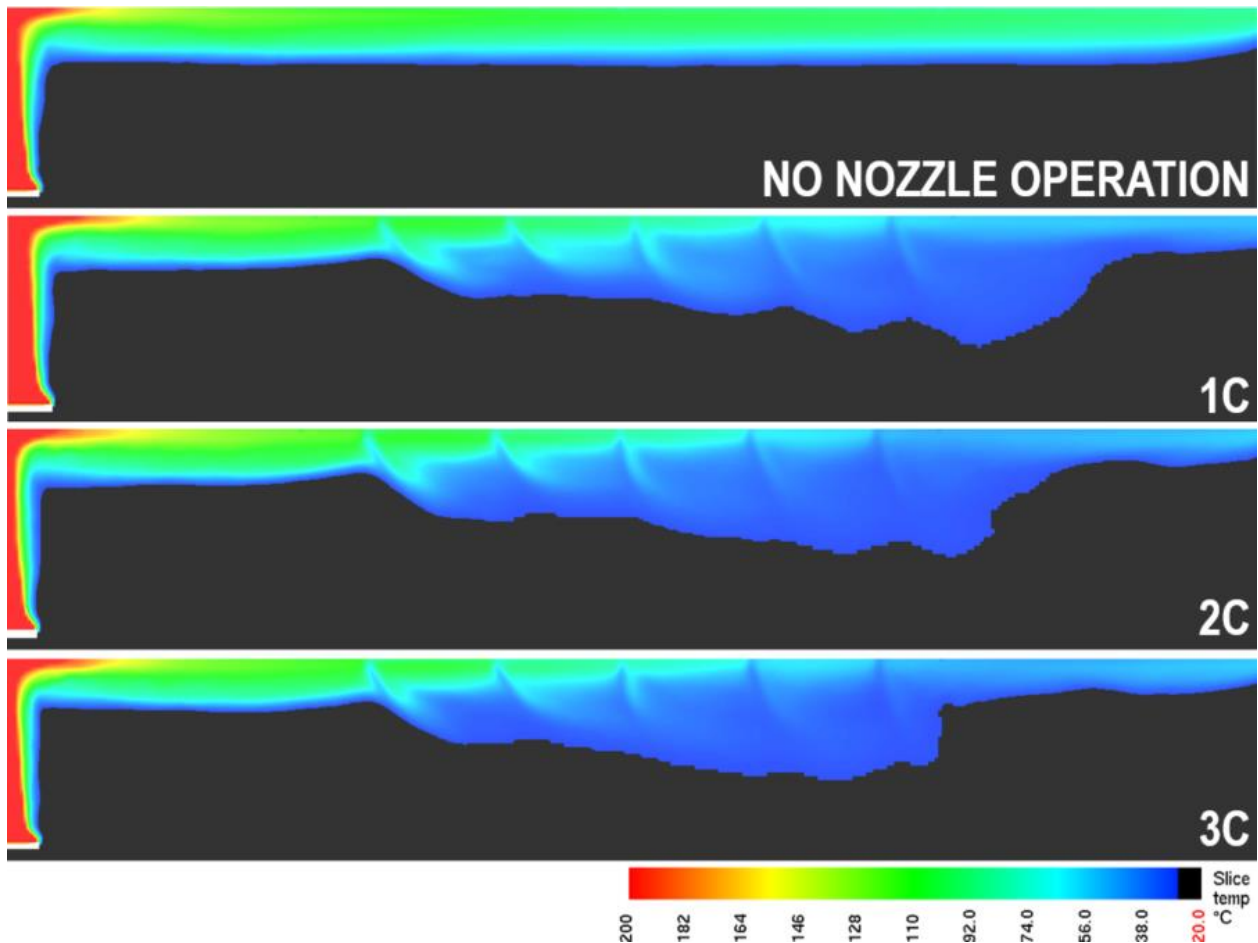
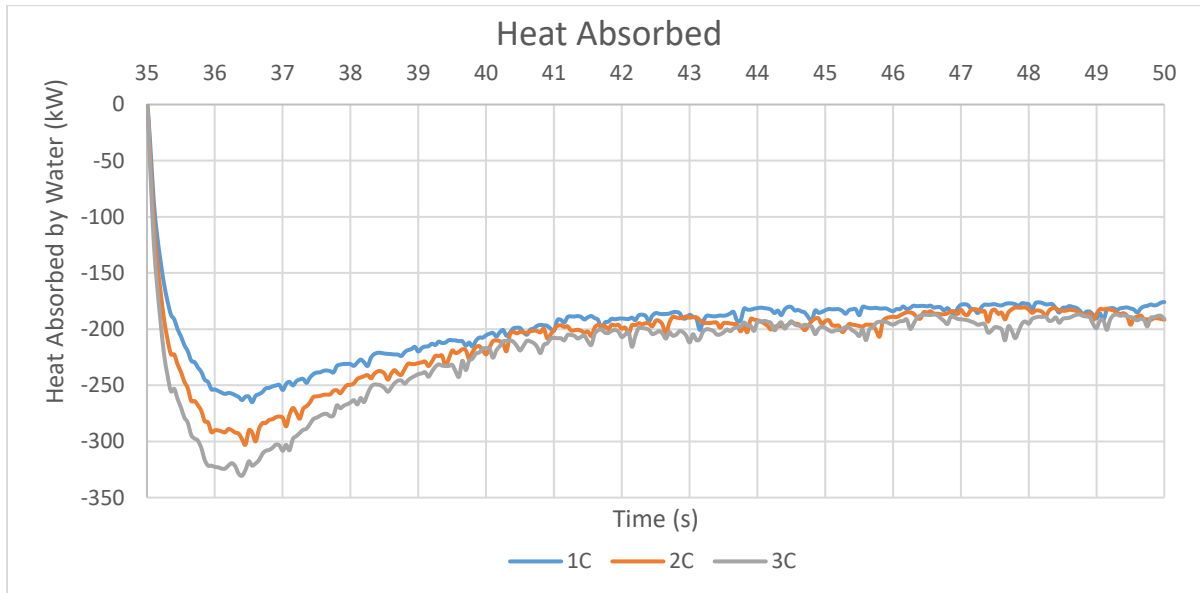


Figure 10: Comparison of the Longitudinal Tunnel Temperature

In the Graph 9 it is possible to identify the differences between the heat absorbed by the water in each nozzle configuration. The configuration with the lowest injection pressure presents the lowest

heat absorbed, while on the other hand, the configuration with the highest injection pressure present the highest heat absorbed.



Graph 9: Heat absorbed by the droplets at different pressures

Finally, in the Table 16 it is possible to see the variations in the heat absorbed according the variations of the system variables. It is agreed that the change in the heat absorbed is proportional to the change in the system variables, but it is not a strongly difference between the numerical results.

Table 16: Impact on the Results according Changes in Variables

Label	Pressure	Flow	Heat Absorbed
1C	55.55%	87.20%	89.60%
2C	77.70%	91.94%	95.24%
3C	100%	100%	100%

Spray Nozzles & Fire with Longitudinal Ventilation

The time modelling of the simulations that consider the interaction of the fire, the longitudinal ventilation and the water spray system will include the 128 seconds required for the back-layering distance and the 8 seconds for the spray system. Therefore, for this simulation it will be considered a total modelling time of 200 seconds, including the activation of the nozzles at the second 180 until the end of the simulation.

Figure 11 presents a set of images where the longitudinal view of temperature across the tunnel is plotted for the different nozzle configurations. As it is possible to see, the configuration without the nozzles operating present a smoke layer considerable thicker when any nozzles configuration is running.

In contrast, in relation to the three different nozzles configuration, it is possible to see that, when the highest injection pressure has been used, the smoke layer becomes thinner than the rest of the nozzle

configuration. Therefore, for 3C1 configuration (0.9 MPa of injection pressure), it is possible to say that the water exerted by the nozzles keeps the smoke layer higher than the other two configurations.

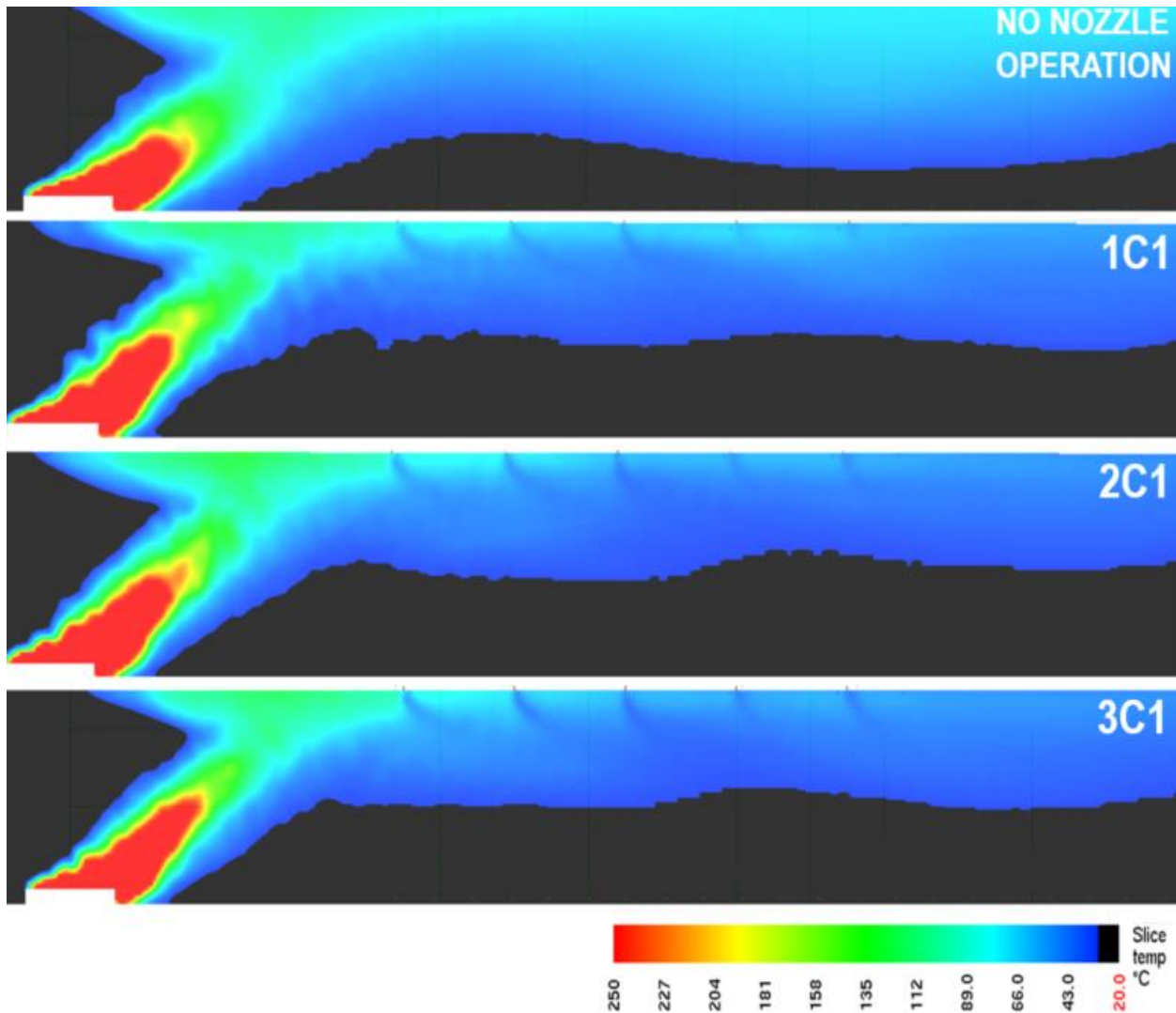
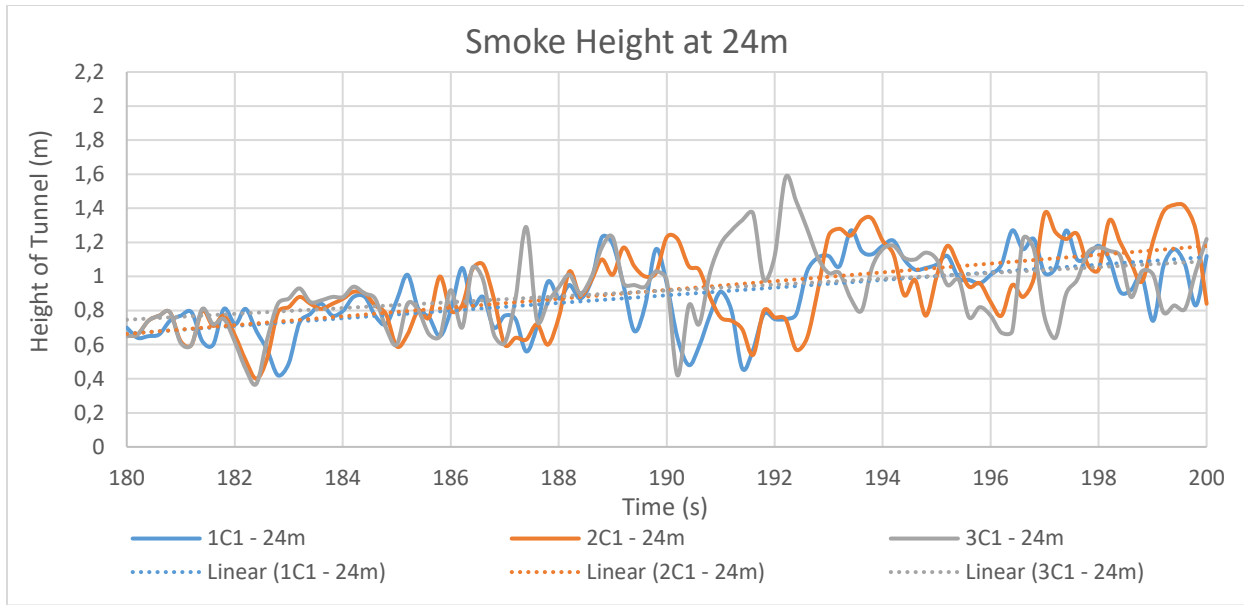


Figure 11: Temperature Slices of the Interaction between Droplets and Longitudinal Ventilation

The following set of graphs present the height of the smoke in the different nozzles configuration at several locations of the tunnel and the results only consider the operation time of the nozzles (from 180 seconds until 200 seconds).

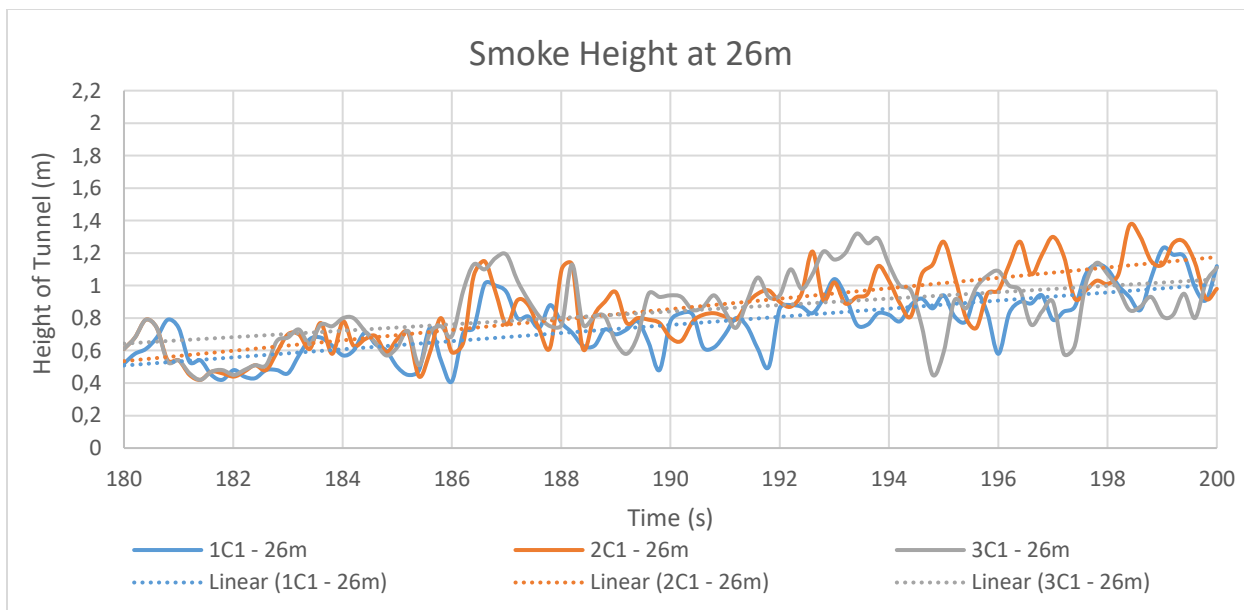
Each set of plotted values have been drawn with a tendency line, allowing a better understanding of the results. In all the graphs and cases, the values are oscillating in time because the flow inside the tunnel is not laminar and there is a turbulent mixing when the fire smoke is pushed back by the longitudinal ventilation.

Graph 10 presents the results measured at 24m along the tunnel. At this position, three lines show that the smoke layer has been elevated from the initial height. Thus, the nozzle configuration 2C1 and 3C1 have the best performance regarding with the increase of the average free smoke height, which one correspond to an average of 0.5m.



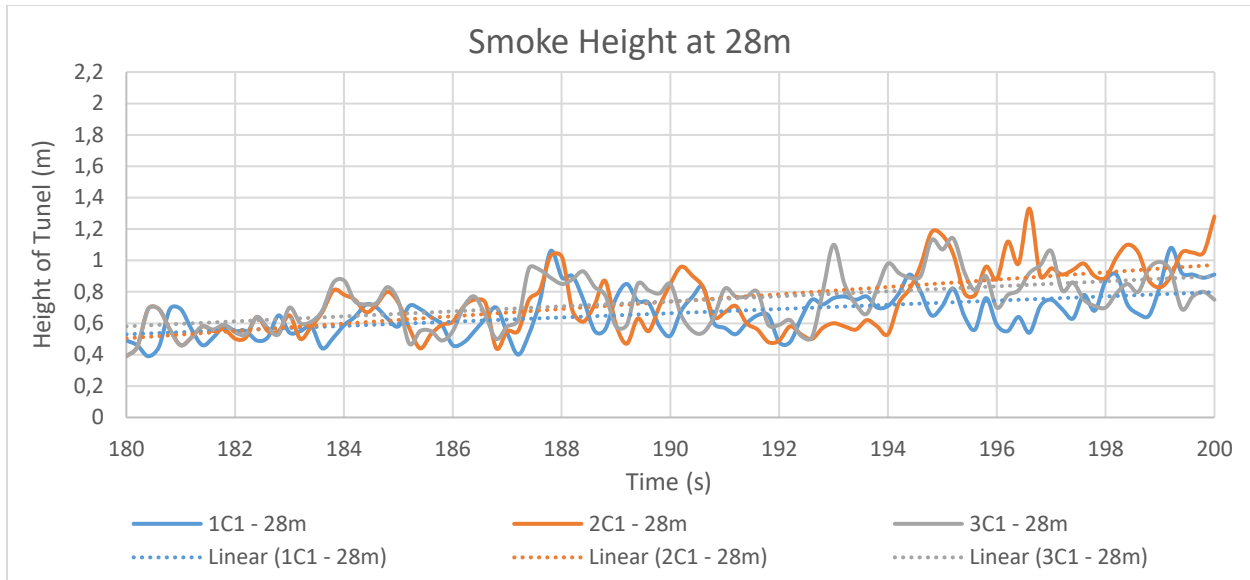
Graph 10: Smoke Height Comparison at 24m

Graph 11 presents the results measured at 26m along the tunnel. At this position, the three lines show that the smoke layer has been elevated from the initial height. Thus, the nozzle configuration 2C1 and 3C1 have the best performance regarding with the increase of the average free smoke height, which one correspond to an average of 0.6m.



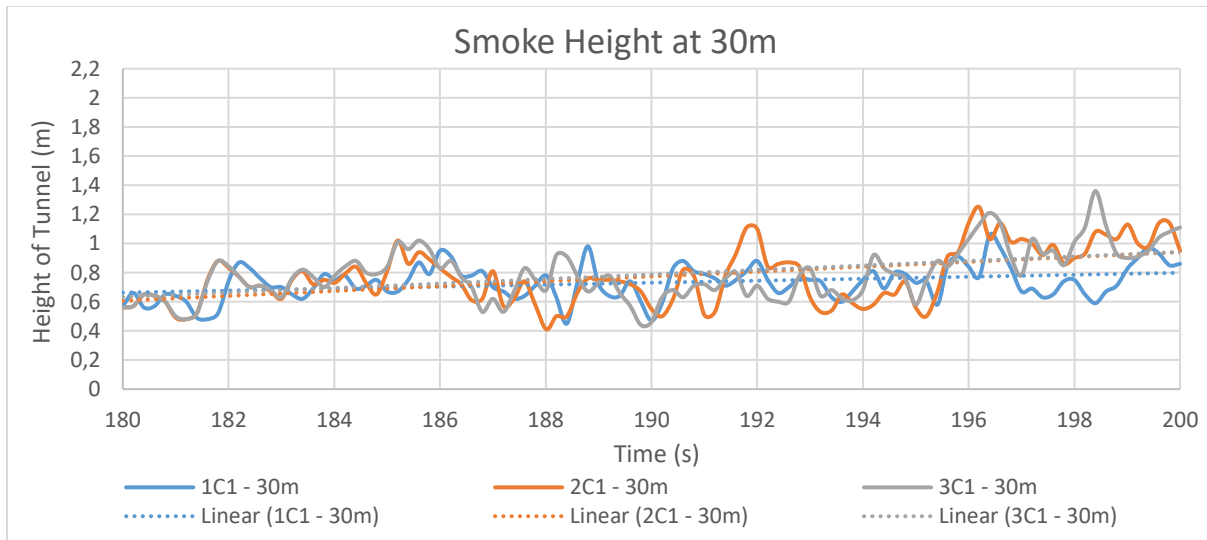
Graph 11: Smoke Height Comparison at 26m

Graph 12 presents the results measured at 28m along the tunnel. At this position, three lines show that the smoke layer has been elevated from the initial height. Thus, the nozzle configuration 2C1 and 3C1 have the best performance regarding with the increase of the average free smoke height, which one correspond to an average of 0.4m.



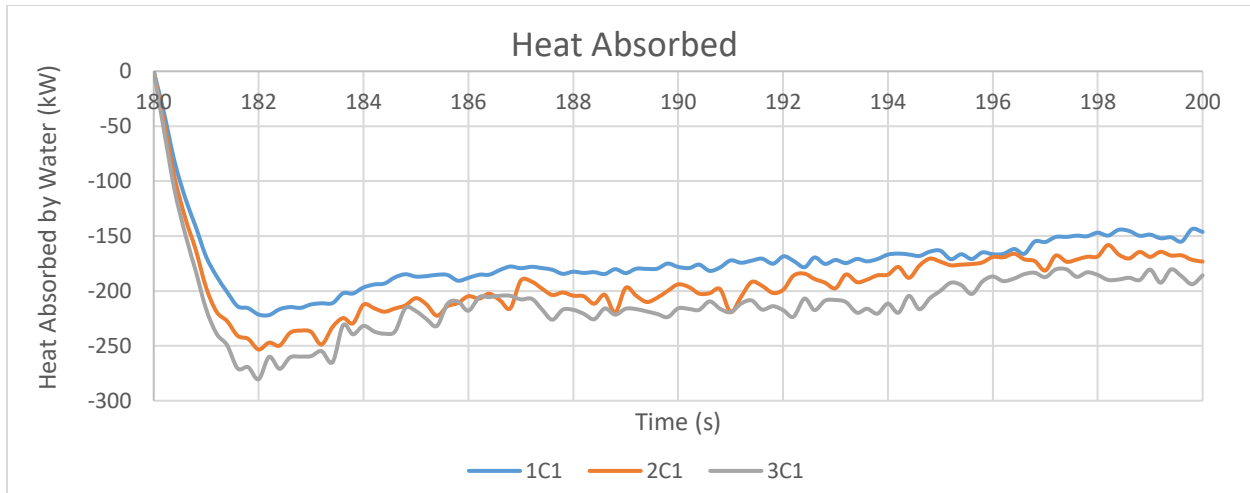
Graph 12: Smoke Height Comparison at 28m

Graph 13 presents the results measured at 30m along the tunnel. At this position, the three lines show that the smoke layer has been elevated from the initial height. Thus, the nozzle configuration 2C1 and 3C1 have the best performance regarding with the increase of the average free smoke height, which one correspond to an average of 0.3m.



Graph 13: Smoke Height Comparison at 30m

In the Graph 14 it is possible to identify the differences between the heat absorbed by the water in each nozzle configuration. The configuration with the lowest injection pressure presents the lowest heat absorbed, thus, the configuration with the highest injection pressure presents the highest heat absorbed.



Graph 14: Heat absorbed by the droplets at different pressures and with longitudinal ventilation

Table 17: Impact on the Results according Changes in Variables

Label	Pressure	Flow	Heat Absorbed
1C1	55.55%	87.20%	82.30%
2C1	77.70%	91.94%	91.80%
3C1	100%	100%	100%

CONCLUSIONS

As a general analysis:

- According to the mesh sensitivity analysis, the most accurate results correspond to the refined mesh. However, the fine mesh can be still used for calculations allowing to reduce the computational time, with variations in the results between 0.1% and 5%.
- The use of water discharge devices in stratified smokes as tunnel fires, it drags down the smoke layer, break down the stratification zone and decrease the height of fresh air.
- As higher is the injection pressure, the heat absorbed from the smoke layer is larger.
- When the longitudinal ventilation system is operating, the average free smoke height corresponds to 0.6m. On the other hand, when the spray nozzle system is activated, the average free smoke height increases from 0.6m average to 0.8-1.0m average.

Evaluating the interaction of the spray nozzles and the longitudinal ventilation, it is possible to argue that:

- The nozzle system with the lowest injection pressure present the lowest increment in the smoke free height.
- The arrangement of spray nozzles with 0.7 and 0.9 MPa present the best performance related with the increment in the smoke free height.

- The spray nozzle system with 0.7 and 0.9 MPa increase an average of 0.45m the smoke free height.
- Although the systems simulated have changed the injection pressure in 22% approximately and the flow in 10% approximately, the heat absorbed have only changed in 6% approximately. Therefore, the scenarios simulated are unresponsive with regards to the flow and pressure variations.

Regarding with the heat absorbed:

- Without the longitudinal ventilation working, the systems simulated have changed the injection pressure in 22% approximately and the flow in 10% approximately, the heat absorbed have only changed in 6% approximately.
- With the longitudinal ventilation working, the systems simulated have changed the injection pressure in 22% approximately and the flow in 10% approximately, the heat absorbed have only changed in 9% approximately.
- Therefore, it is possible to state that the scenarios without the longitudinal ventilation are unresponsive with regards to the flow and pressure variations.
- The heat absorbed by the water when the longitudinal ventilation is working is higher than the system operating without the ventilation system.
- One of the reasons why the simulations of the spray nozzles operating with the longitudinal ventilation absorb more heat, it could be due to the turbulence in the flow generated by the ventilation system.

Regarding with Tunnel Safety:

- The use of water discharge devices in stratified smokes as tunnel fires, it drags down the smoke layer, break down the stratification zone and decreasing the height of fresh air. By this way, the occupants could be affected by the smoke, hot gases, or irritants-toxics gases.
- On the other hand, when water discharge devices in stratified are used, it is possible to decrease the temperature of the hot gases.
- Combining the longitudinal ventilation with a system of spray nozzles could allow to decrease the air temperature downstream from the fire. Hence, the structure, components and others would present lower temperatures and could avoid thermal damage.
- Despite that the longitudinal ventilation system in a tunnel are designed to fulfil life evacuation criteria upstream from the fire, the combination with the spray nozzles would improve the tenability conditions downstream from to fire for the people, tunnel operators or firefighters.

REFERENCES

Lehtimäki, M. (2017). Simulation of Water Cooling in Fires. Aalto, Finland. School of Engineering Aalto University.

Boerstlap, G. & Hoste, K. (Version 1.1). HPC Tutorial for Windows Users. VSCentrum Belgium. Vlaams Supercomputer Centrum.

Society Fire Protection Engineers. (2016, fifth edition). SFPE Handbook of Fire Protection Engineering. Greenbelt, MD, USA. Springer.

National Institute of Standards and Technology. (2017, sixth edition). Fire Dynamics Simulator User's Guide. USA. U.S. Department of Commerce.

Wang, J. & Nie, Q. & Tang, Z. (2017). CFD Simulations of the Interaction of the Water Mist Zone and Tunnel Fire Smoke in Reduced-scale Experiments. 8th International Conference on Fire Science and Fire Protection Engineering, 2017, Procedia Engineering 211, pp. 726-727.